Neutron-rich Nuclei at and Beyond the Dripline in the Range Z=4 to Z=10 Studied in Kinematically Complete Measurements of Direct Reactions at Relativistic Energies

The R3B Collaboration
Spokesperson: T. Aumann (GSI)

Abstract.

We propose to study light neutron-rich nuclei (Z=4 to Z=10) utilizing kinematically complete measurements of reactions at relativistic energies with the LAND/R3B reaction setup at Cave C. The physics topics to be studied comprise the measurement of astrophysical reaction rates relevant for r-process nucleosynthesis using heavy-ion induced electromagnetic excitation and quasi-free knockout reactions to study the evolution of shell and cluster structures close to and beyond the dripline. Concerning the latter topic, the evolution of neutron shells is studied in (p,pn) reactions and the evolution of alpha clustering in the ground states of Be isotopes as a function of increasing neutron number is investigated in (p,pα) reactions. Unbound (ground and excited) states will be populated and identified in (p,2p) reactions. Finally, the quenching of single-particle strength in neutron-proton asymmetric nuclei will be addressed by knocking out deeply bound protons and neutrons in (p,2p) and (p,pn) reactions for nuclei with varying neutron-proton asymmetry. The same setup will be used for all reactions making very efficient use of the allocated beam time. In total, we ask for 21 days of beam time.

1. Measurements of (n,γ) Rates of Light Neutron-Rich Nuclei for R-Process Nucleosynthesis

The search for the astrophysical site of r-process nucleosynthesis remains one of the most exciting challenges in nuclear astrophysics. Recent observations of metal-poor halo stars [Sne03] even support the possibility of contributions from two r-process components, related to different stellar events. The observed abundances of elements heavier than barium (A>130) are very similar to the solar r-abundance pattern, whereas for lighter elements deficits are observed. This finding suggests the existence of a very robust r-process mechanism, which is independent of the metallicity of the progenitor star. A promising candidate for such a scenario is the neutrino-driven wind model of core collapse supernovae [Mey92, Woo94]. There, the r-process takes place close to the newly formed neutron star, where the neutrino driven wind removes neutron rich matter from the surface of the proto-neutron star. In this region the entropy is so high that all the previously existing nuclei are destroyed and only the lightest nuclei such as neutrons, protons, and α-particles survive. This could explain quite naturally why the r-process is independent of metallicity. During the fast expansion of matter, the seed nuclei for the successive r-process are formed by charged-particle-induced reactions, the so-called α-capture process. This early phase is crucial for an effective r-process since it defines the neutron-to-seed ratio. A high neutron-to-seed ratio is mandatory for a successful production of heavy nuclei during the r-process. But not only charged particle reactions are important. It was shown [Ter01] that the reaction flow through very light, neutron-rich nuclei which is established during the expansion phase can also produce seed nuclei, especially within models with short dynamical expansion time scales. Therefore, an extension of the r-process network towards light neutron-rich nuclei compared to previous works [Mey92, Woo94] was implemented, resulting in changes of the final abundances of the heavy-elements by as much as an order of magnitude. The exact nucleosynthesis path, however, depends on the reaction rates, which are only poorly known for nuclei of interest. Especially for the neutron-rich nuclei close to the drip-line experimental information is scarce. Therefore, [Sas05] studied the sensitivity of r-process nucleosynthesis on 18 light-element reaction rates and identified the most crucial ones. Concerning neutron capture cross sections they identified (n,γ)-rates of neutron-rich carbon isotopes as the most important ones, since these lie on the main flow-paths to heavier nuclei:

$$^{15}\mathrm{C}(n,\gamma)^{16}\mathrm{C}(n,\gamma)^{17}\mathrm{C}(n,\gamma)^{18}\mathrm{C}\begin{bmatrix}(\alpha,n)^{21}\mathrm{O}(n,\gamma)^{22}\mathrm{O}(n,\gamma)\\(e^{-}\nu)^{18}\mathrm{N}(n,\gamma)\ldots^{23}\mathrm{N}(e^{-}\nu)\end{bmatrix}^{23}\mathrm{O}$$

$$^{15}\mathrm{C}(n,\gamma)^{16}\mathrm{C}(e^{-}\nu)^{16}\mathrm{N}(n,\gamma)\ldots^{23}\mathrm{N}(e^{-}\nu)^{23}\mathrm{O}$$

$$^{23}\mathrm{O}(n,\gamma)^{24}\mathrm{O}\begin{bmatrix}(\alpha,n)^{27}\mathrm{Ne}\ldots\\(e^{-}\nu)^{24}\mathrm{F}\ldots\end{bmatrix}$$

The only way to obtain information on neutron capture rates of such short-lived, neutron-rich nuclei is to measure the time-reversed reaction via Coulomb Dissociation, and then apply the principle of detailed balance. Therefore, we propose to measure (n,γ) rates on neutron-rich carbon isotopes, in particular ^{17}C(n,γ)^{18}C, because ^{18}C resembles a kind of waiting point for the nucleosynthesis flow towards heavier nuclei. However, with a primary beam of ^{40}Ar and FRS settings for ^{18}C we will get the nuclei ^{15}B, ^{14}B, ^{12}Be, and ^{11}Be as contaminants with even higher rates than ^{18}C. This means that we can also measure, as a by-product, some of the rates which are important for the reaction path leading to ^{15}C:

$$\alpha(\alpha n,\gamma)^{9}\mathrm{Be}\begin{bmatrix}(\alpha,n)^{12}\mathrm{C}(n,\gamma)^{13}\mathrm{C}(n,\gamma)\\(n,\gamma)^{10}\mathrm{Be}(\alpha,\gamma)\end{bmatrix}^{14}\mathrm{C}(n,\gamma)^{15}\mathrm{C}$$

$$\alpha(t,\gamma)^{7}\mathrm{Li}(n,\gamma)^{8}\mathrm{Li}(\alpha,n)^{11}\mathrm{Be}(n,\gamma)^{12}\mathrm{Be}(n,\gamma)^{13}\mathrm{Be}(n,\gamma)^{14}\mathrm{Be}(n,\gamma)^{15}\mathrm{Be}(e^{-}\nu)^{15}\mathrm{C}$$

Rate estimates were calculated with the Lise++ code with parameters shown in Table 1 and the resulting secondary beam intensities can be seen in Table 2. The rate estimates are based on production cross sections calculated with EPAX 2.15 [Sum00]. A comparison with experimental data from [Oza00] shows that the calculations underestimate the cross sections for carbon isotopes in general. For ^{18}C, the measured production cross section is a factor of 6 larger than the EPAX 2.15 value.

If we assume an average cross section of 10 mb/MeV for the excitation energy region from 0 to 1 MeV above threshold, we expect a count rate of 700 counts/MeV (140/bin in average) in 10 shifts (input: 2 g/cm^2 Pb, 50% overall efficiency, experimental production cross section).

2. The Quasifree Scattering Programme

2.1. Shell Structure and Quenching of Single-Particle Spectroscopic Factors in Bound Exotic Nuclei

2.1.1 Summary

We propose to use the quasifree (p,2p) and (p,pn) reactions with radioactive beams in inverse kinematics to measure spectroscopic information for the valence and deeply bound neutrons and protons of the complete Oxygen isotopic chain. This will allow us to study the evolution of the $\pi 1p_{1/2}$, $\pi 1p_{3/2}$ and $\pi 1s_{1/2}$ proton single-particle states with the (p,2p) reaction and the $\nu 2s_{1/2}$, $\nu 1d_{5/2}$, $\nu 1p_{1/2}$, $\nu 1p_{3/2}$ and $\nu 1s_{1/2}$ neutron single-particle states with the (p,pn) reaction. Information will also be obtained on other nuclei in this region that are produced in the same FRS settings, such as F and Ne. In addition to the intrinsic interest for the structure of exotic nuclei, the absolute spectroscopic factors we will extract will allow us to systematically study the dependence of the valence and deeply bound nucleon occupancies on isospin asymmetry. A strong dependence has been suggested from recent measurements using one-nucleon removal (and transfer) reactions at MSU, GANIL and GSI. However, the results are highly controversial as such behaviour is not found from (e,e'p) reactions (which are however restricted to stable nuclei) and the dependence is much stronger than that predicted by advanced many-body calculations of asymmetric nuclei and nuclear matter. Measurements using a reaction known to be able to provide absolute spectroscopic factors are urgently needed to establish this dramatic behaviour. The proposed measurements will enable us to investigate this topic.

2.1.2 Background

Recently, the validity of the mean-field picture of nuclei and how this picture is modified by long- and short-range correlations has been challenged on several fronts by theoretical and experimental studies of exotic nuclei. Exotic nuclei are asymmetric systems where, for example, N>>Z. Such large variations in isospin are predicted to modify the mean field itself and also the long-range and short-range correlations. One consequence is the evolution of the shell gaps and magic numbers with isospin. Mean-field changes will arise as the nuclear surface evolves towards diffuse neutron matter. The derivative of the mean field-potential will therefore become weaker, reducing the spin-orbit interaction. The role of certain residual interactions becomes enhanced with proton-neutron asymmetry, in particular the monopole interaction that acts between proton-neutron spin-orbit partners. The combination of these effects will mean that the traditional shell gaps and magic numbers will disappear and new ones will appear. Dramatic examples of this phenomena have already been found experimentally in the light neutron-rich nuclei, where the N=8 and N=20 shell closures vanish and new shell closures appears at N=14 and N=16. A manifestation of this is that the dripline is reached already in the Oxygen isotopes at ^{24}O and ^{28}O is unstable. Another consequence is that the occupancies themselves will become isospin dependent. Such an effect has recently been predicted theoretically using sophisticated many-body techniques such as Self-Consistent Green's Function theory. There is also some limited experimental evidence that this is the case. Recently, one-nucleon removal experiments have shown that the occupancies of valence states in neutron-halo nuclei appear close to unity as expected in very low-density nuclear matter. Conversely, a one-nucleon removal experiment has measured a spectroscopic factor for the deeply-bound $\nu(0d_{5/2})$ neutron state in the proton-rich nucleus ^{32}Ar that is only

24% of that predicted by the many-body shell model. This may be evidence for the strong depletion of occupancies of deeply-bound neutrons in proton-rich nuclei, although the interpretation of the data is still very actively debated amongst the international community.

The most precise information on single-particle properties of nuclei comes from proton- and electron-induced quasifree scattering reactions. Fig. 1 shows, as an example, spectral functions extracted from $^{16}O(e,e'p)$ reactions [Mou80]. One can easily identify the different single-particle states. The corresponding momentum dependence is also shown exhibiting the typical behaviour for the different angular momenta involved. From the integrated strength, spectroscopic factors or occupation probabilities may be derived. To extract such complete information on the single-particle structure of exotic nuclei is our final goal. The reduction of single-particle strength due to short-range, tensor and long-range correlations has been established for stable nuclei mainly from electron- and proton-induced quasifree scattering reactions to be on the order of 0.6 to 0.7. Fig. 2 shows a compilation of experimental results as a function of the difference in separation energies for neutron and protons. The (e,e'p) results for stable nuclei appear around $\Delta S=0$ with a quenching factor of about 0.6.

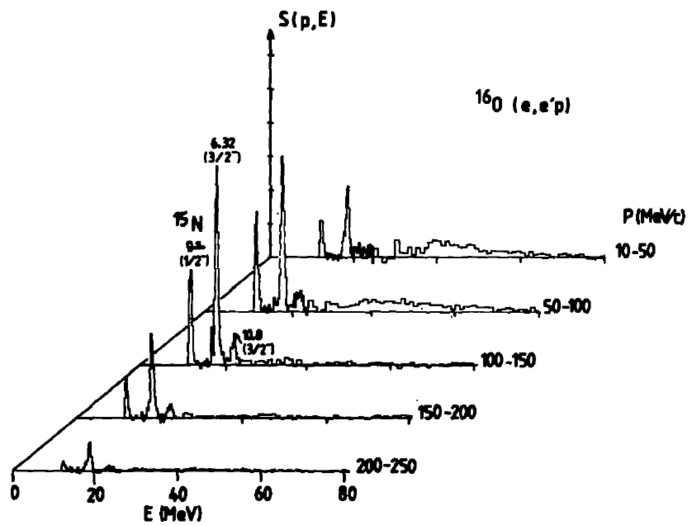

Figure 1. Spectral functions obtained from electron-induced proton knockout experiments [Mou80].

Recently, spectroscopic factors have been extracted from one-nucleon removal reactions with radioactive beams using light nuclear targets, such as C and Be at MSU, GANIL and GSI. A compilation of the results [Gad08] are shown in Fig. 2, together with the (e,e'p) results. They suggest a much stronger suppression of single-particle strength for deeply bound nucleons in isospin asymmetric systems, while the loosely bound valence neutrons in neutron-rich nuclei appear to have spectroscopic factors very close to unity, as expected in very low-density nuclear matter. The reason for this isospin dependence is an open and debated question. For example, the dependencies of both short- and long-range correlations on isospin asymmetry in infinite nuclear matter have been studied within various many-body frameworks [Fri05]. Recently, the results of a study of nuclei with large proton-neutron asymmetry using the self-consistent Green's functions method and based on the chiral N3LO force, have shown an asymmetry dependence of the spectroscopic factors similar to that observed experimentally but considerably weaker in magnitude [Bar08]. Further experimental and theoretical studies are clearly needed. Since we cannot at present do electron induced quasifree scattering with exotic nuclei, quasifree scattering of exotic nuclei on a hydrogen target provides us with the unique opportunity to probe in detail the single-particle strength in very asymmetric nuclear systems.

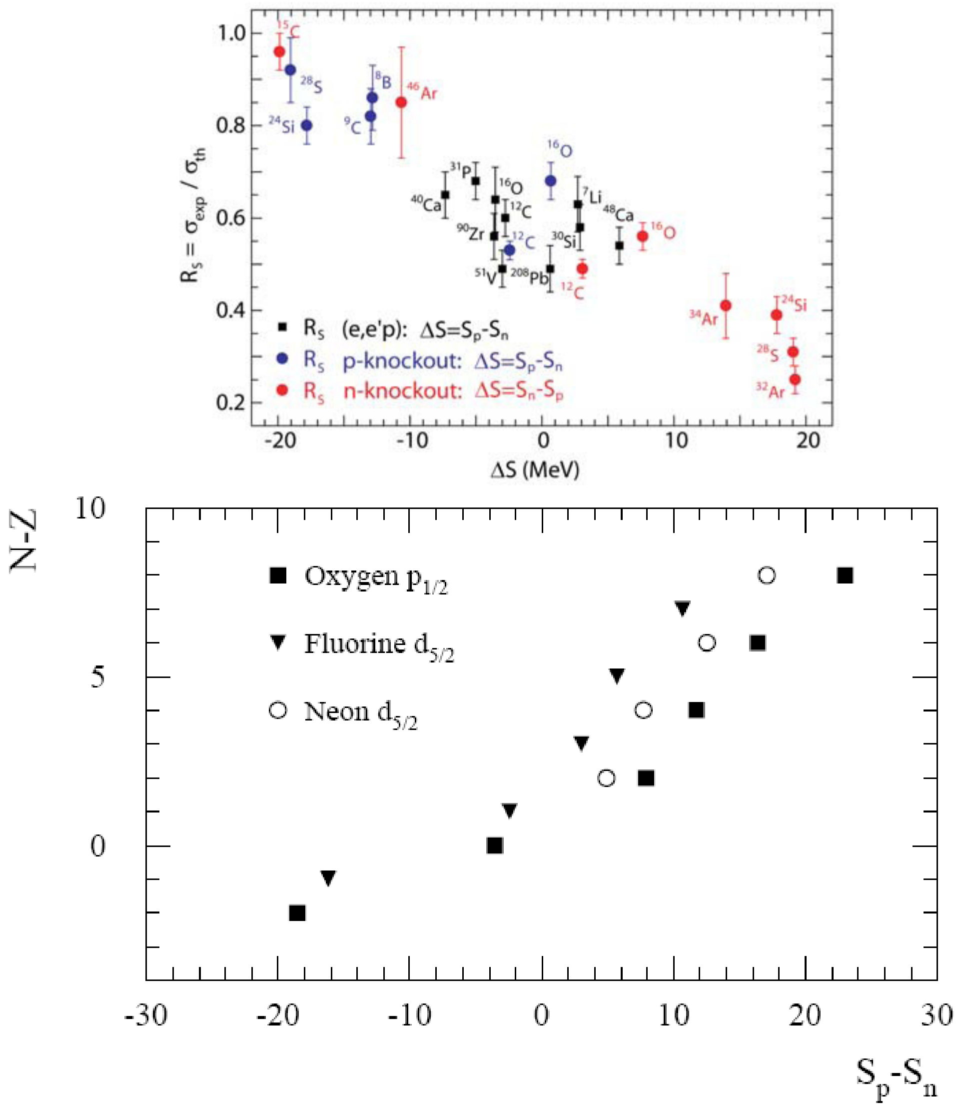

Figure 2. Upper panel: Reduction of spectroscopic factors observed in different nucleon knockout reactions as a function of the difference in separation energies of the two nucleon species [Gad08]. Lower panel: Neutron-proton asymmetry N-Z versus the separation-energy difference (same scale as figure above) of protons from different shells for the O, F and Ne nuclei to be studied. Not shown are the even deeper lying $p_{3/2}$ and $s_{1/2}$ protons, which have larger S_p-S_n values for the same neutron-proton asymmetry N-Z. A similar picture can be drawn for the neutron states, which will be measured as well in (p,pn) reactions.

2.1.3 Proposed Measurements

The main focus of the experiment is to perform quasifree scattering measurements – such as (p,pn) and (p,2p) – with a CH_2 target. This will thus be one of the first such experiments with high-energy radioactive beams and a precursor to the future quasifree scattering studies at R^3B. For the reaction to be quasifree, the beam energy needs to be relatively high, and thus this type of reaction is ideally suited for the beam energies available at GSI. In inverse kinematics, the bound nucleon in the projectile is knocked out via quasifree nucleon-nucleon scattering with a proton in the target, and a hole state is produced as a residual nucleus. By measuring the four momenta of the two nucleons in the final state, the separation energy and momentum of the knocked-out nucleon are obtained. Because we measure in inverse kinematics, we can also measure the recoil momentum distribution of the residual projectile-like nucleus *directly*. In the (p,2p) quasifree scattering studies this will give us the unique possibility of precisely investigating the effects of final state interactions, or re-scattering, of the protons as they exit the nucleus by comparing the recoil momentum distribution reconstructed from the two outgoing protons and the distribution measured directly. A full understanding of this process is of great importance in the analysis of quasifree scattering. It is normally accounted for in the theoretical descriptions by using distorted waves and this is a major source of uncertainty in the theoretical descriptions of the reaction mechanism. Such an investigation is not possible in normal kinematics and so our studies will provide important new information on the quasifree scattering reaction process in general. Recent quasifree scattering test experiments with beams of ^{12}C, ^{17}Ne and Ni isotopes performed by our collaboration using the Cave C setup have successfully demonstrated that this type of experiment is feasible.

We intend to investigate the spectroscopy of the valence and deeply bound protons and neutrons of the complete Oxygen isotopic chain, from ^{14}O at the proton dripline to ^{24}O at the neutron dripline, using (p,2p) and (p,pn) reactions, respectively. This will allow us to study the evolution of the $\pi 1p_{1/2}$, $\pi 1p_{3/2}$ and $\pi 1s_{1/2}$ proton single-particle states with the (p,2p) reaction and the $\nu 2s_{1/2}$, $\nu 1d_{5/2}$, $\nu 1p_{1/2}$, $\nu 1p_{3/2}$ and $\nu 1s_{1/2}$ neutron single particle states with the (p,pn) reaction. Information will also be obtained on other nuclei in this region that are produced in the same FRS settings, such as F and Ne. We will also investigate the quenching of proton and neutron single-particle strength along the O, F and Ne isotopic chains. In our experiment, we can extract the excitation energy of the hole state in two ways. We may reconstruct the energy from the measurement of the proton angles and energies (as in a 'classical' quasi-free scattering experiment) or by observing the produced fragment. In the latter case, the gamma decay of excited states in the A-1 fragment is detected in coincidence. In addition, we can reconstruct also unbound states using the invariant-mass method. The proposed experiment will thus be sensitive to the full energy range as depicted in Fig. 1. The lower part of Fig. 2 shows the correlation of the binding-energy difference S_p-S_n (same scale as upper figure) with the neutron-proton asymmetry, N-Z. As can be seen, the knockout from different shells in the isotopic chains of O, F and Ne will allow us to vary the isospin as well as the asymmetry in separation energy. The full range in binding-energy asymmetry from -20 MeV to 20 MeV will be covered.

It should be noted that the FRS settings foreseen to cover above mentioned isotopes will contain at the same time other interesting nuclei to study in the mixed beam. We mention here the one-neutron halo nuclei ^{11}Be and ^{15}C, which have been studied in the past by other methods. Here, we can investigate breakup reactions of halo nuclei under quasifree conditions in a kinematically complete measurement of (p,pn) reactions.

2.2 Nuclei Beyond the Neutron Dripline

The delineation of the neutron dripline and the handful of studied cases beyond it have proven highly interesting. The extreme clustering, disappearance of magic numbers etc found in many of the dripline nuclei continues into the unbound region. One evident example is the termination of the chain of bound oxygen isotopes at N=16, well before the doubly-magic ^{28}O. A recent experiment [Aks08] has shown that proton-knockout reactions can be used to populate unbound systems one and even two steps beyond the last bound Lithium isotope, in spite of the neutron excess and small binding energy of the original nucleus. Thus, we would propose to take this method to two further regions of the nuclear chart, namely the unbound systems in the beryllium/boron and oxygen chains.

The method of choice is high-energy proton knock-out reactions in inverse kinematics. The same experimental dataset will be useful for several approaches; the cleanest reaction channel is obtained by exclusive (p,2p) reactions where the existing proton tracking devices will be able to select events satisfying QFS conditions. Nevertheless, we have also successfully performed similar studies on carbon targets [Mei02], indicating that a CH_2-target together with a carbon target can be used for (p,2p) exclusive reactions on the hydrogen content in the CH_2 target and inclusive reactions on carbon targets. For the cases with sufficient statistics in the exclusive case, corrections by using a pure carbon target will possibly be needed which for the inclusive measurements (on either C and CH_2 targets) will increase the total statistics.

2.2.1 The ^{25}O Case

The neutron unbound ground state of ^{25}O was recently observed for the first time [Hof08] in a proton knock-out reaction from a ^{26}F beam and beryllium target. One single resonance was observed in the ^{24}O+n relative-energy spectrum, corresponding to a neutron decay energy of 770 keV, with a total width of 172(30) keV. The N=16 shell gap was established to be 4.86(13) MeV by the energy difference between the $1s_{1/2}$ and $0d_{3/2}$ orbitals. The neutron separation energy for ^{25}O agrees with the calculations of the universal *sd* shell model interaction. However, this interaction predicts that the ground state of ^{26}O is bound with a two-neutron energy of about 1 MeV. This is, however, contradicting the experimental data, which show that this nucleus is unbound. The observed decay width was found to be on the order of a factor of 2 larger than the calculated single-particle width using a Woods-Saxon potential. The proposed measurement of the ^{26}F(p,2p)^{25}O reaction will provide improved data in several respects. The reaction will be measured fully exclusive (including γ-ray detection) with better statistics and better resolution. In addition, we expect a sufficient number of events for the population of the ^{26}O ground state in order to estimate its mass and width.

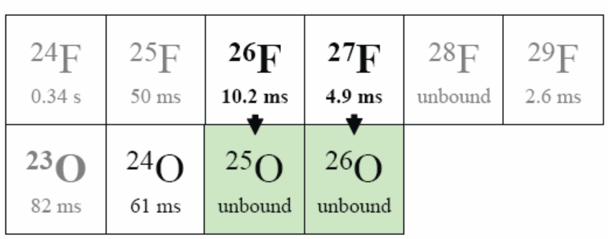

Figure 3. The proposed one-proton knock-out reactions from ^{26,27}F to investigate states in ^{25,26}O.

2.2.2 The ^{16}B case

The ground state of the unbound system ^{16}B has been investigated for the first time [Lec09] via single-proton removal from a 35 MeV/nucleon ^{17}C beam impinging a carbon target. The energy of the decay of ^{16}B by neutron emission was reconstructed. The resulting spectrum exhibited a narrow peak at 85 keV above threshold. It was argued that this feature most probably corresponds to a very narrow (Γ about 100 keV) resonance which decays by d-wave neutron emission.

2.2.3 The ^{13}Be case

The unbound nucleus ^{13}Be has recently been studied at GSI, in one-neutron removal reaction using both carbon [Sim08] and hydrogen targets [Aks09a]. The data reveals that the ^{12}Be+n system have several resonances with seemingly complicated structures. Lack of information on population of the ^{12}Be γ-decaying states prevented a detailed analysis of the data. The main conclusion that can be made is that the interaction between the neutron and the ^{12}Be fragment is much weaker than in the ^{9}Li+n case. Since the structure of ^{13}Be still is a rather open case, data from one-proton removal from ^{14}B, including coincident γ-events, may give important new clues for its understanding.

2.2.4 The ^{15}Be Case

The successful observation of the unbound Lithium isotopes ^{12,13}Li [Aks08] and the Helium isotopes ^{9,10}He [Aks09b] in removal reactions from the exotic beams ^{14}Be and ^{11}Li demonstrated in a powerful manner that the use of relativistic beams may populate even more exotic systems without destroying the exotic cores. We propose to search for ^{15}Be by 2p removal from ^{17}C.

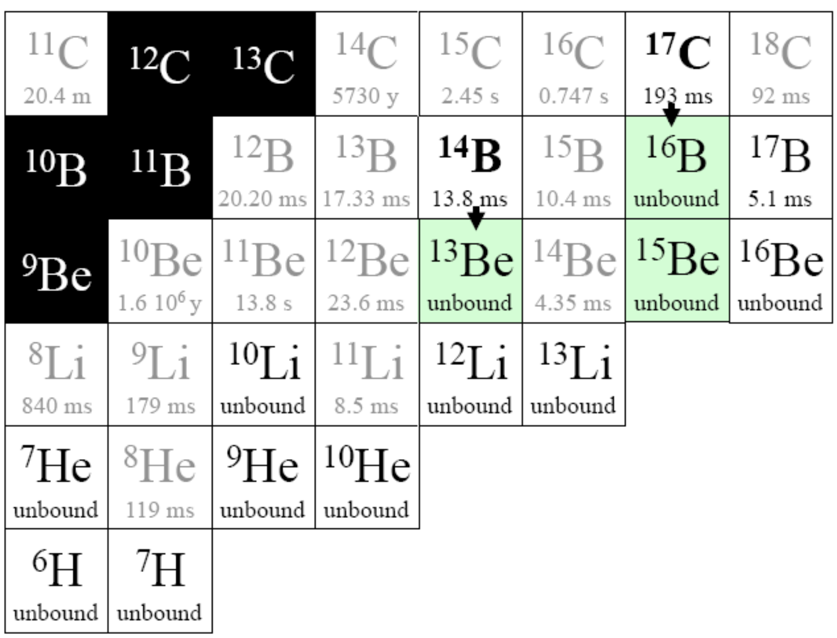

Figure 4. The proposed knock-out reactions from ^{17}C and ^{14}B to investigate the unbound nuclei ^{16}B and ^{13,15}Be.

2.2.5 Two-Proton Knock-Out Reactions

Two-proton knockout from intermediate energy beams of neutron-rich nuclei impinging on light nuclear targets has been shown recently to be a direct reaction capable of producing neutron-rich residues and populating their excited states [Baz03]. The reaction holds great promise for the study of neutron-rich nuclei, for example, ^{12}He can be produced by using ^{14}Be beams or ^{13,15}Li from ^{15,17}B. Two-proton knock-out studies can provide access not only to more exotic nuclei as compared with the one-proton knockout but as well to the ground-state correlation function of the projectile. However, the conclusions made in Ref. [Baz03] need to be confirmed in independent experiments. The existing experimental setup will allow us to obtain the data on two-proton removal channel as a by-product during experiments where the one-proton knock-out reaction is studied. We plan to collect experimental data from the two-proton removal channel in order to study the reaction mechanism itself and to investigate its usage as a tool to go far beyond the dripline. For example the reactions (^{17}C,^{15}Be) and (^{28}Ne,^{26}O) are of great interest as an alternative approach to the (p,2p) reaction. The lower cross section for the two-proton knockout is compensated (or might even be overcompensated) by the higher beam intensities for the projectile.

2.3 Probing the Cluster Structure of Neutron-Rich Beryllium Isotopes

2.3.1 Background

We propose to probe the change in the degree of clustering in the ground-states of the beryllium isotopes as the neutron drip-line is approached using the (p,pα) quasifree scattering reaction. The structure of the Z=4 ground state nuclei offers a rather intriguing possibility. The N=Z nucleus ^{8}Be is unstable against alpha-decay by 92 keV, the finite lifetime of the state being provided by the presence of the Coulomb barrier. Its existence just above the decay threshold facilitates the formation of two alpha-clusters in the ground-state. Such a structure is demonstrated rather well in the *ab initio* Greens Function Monte Carlo calculations [Wir00] (as shown in Fig. 5). These calculations are based around a realistic nucleon-nucleon interaction and have no *a priori* prejudice to clustering, nevertheless the cluster structure emerges.

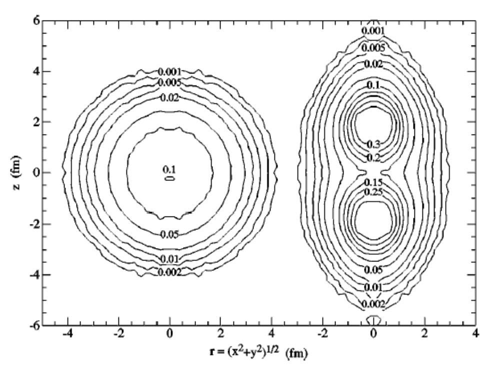

Figure 5. Calculations of the density of ^{8}Be from [Wir00].

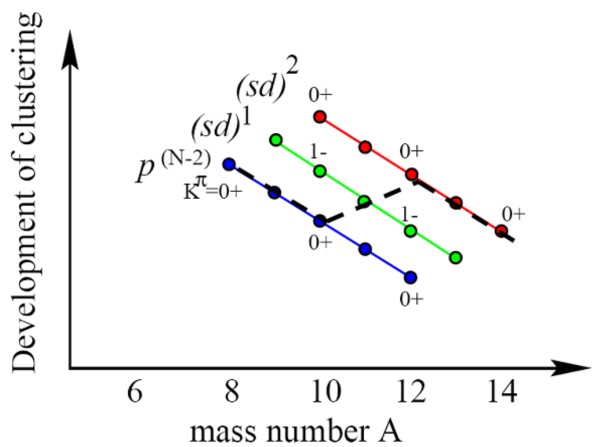

Figure 6. Evolution of the molecular structure of Be isotopes as a function of mass. The dashed line shows the configuration of the ground states. The ^{9}Be ground state has one neutron in the p-orbital (π), and ^{10}Be has a $(\pi)^2$ configuration. ^{11}Be has a single neutron in the sd-shell (σ) and the ^{12}Be ground state $(\sigma)^2$.

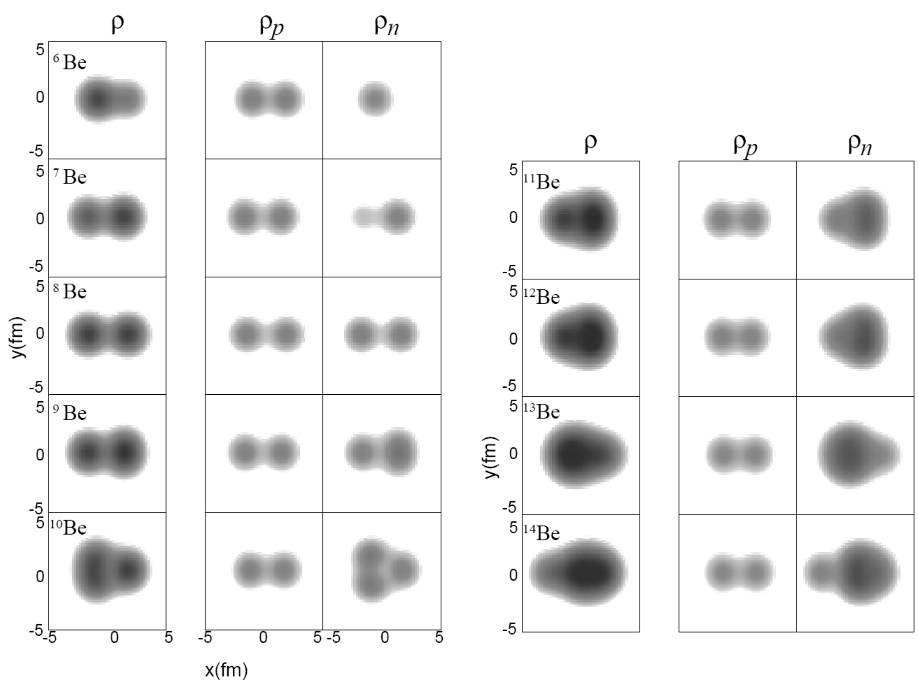

Figure 7. AMD calculations of the density (total, proton and neutron) densities for the Be isotopes. The cluster structure (observed in the proton density) is preserved up to the drip-line [Kan01].

What happens when valence neutrons are added to such a system is a rather interesting question. There are at least two limiting possibilities: i) the presence of the neutrons disrupts the alpha-particles and a more shell-model like structure results, or ii) the two alpha-particles form the basis for the potential in which the neutrons move. The structure of ^{9}Be indicates the latter is the more appropriate description. In this instance the neutron passes from one alpha-particle before being exchanged with its partner – just as electrons are exchanged in atomic molecules. This delocalisation of the neutron reduces the kinetic energy and thus increases the

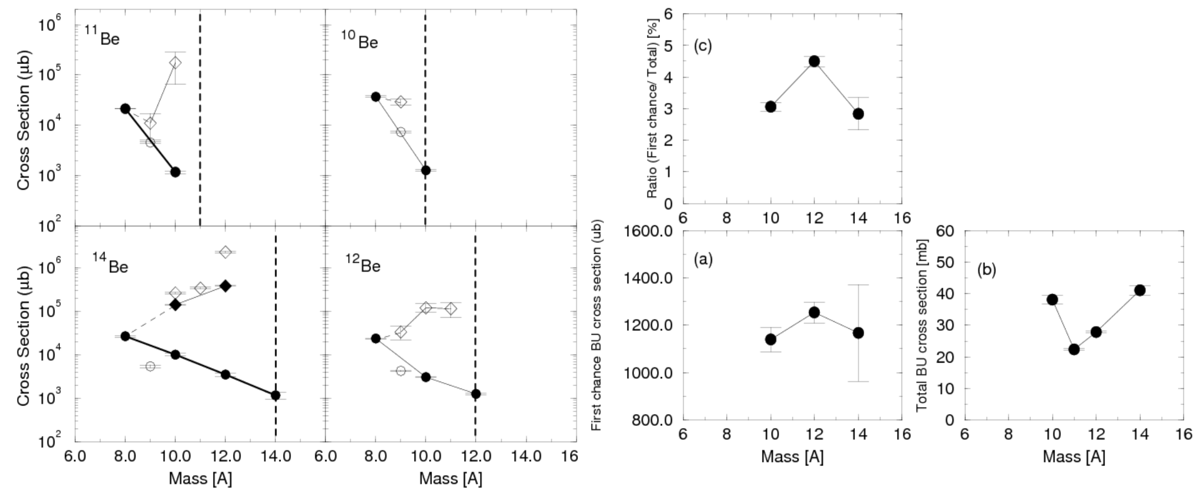

Figure 8. *left* Neutron-removal (open diamonds) and cluster breakup (filled circles) cross sections for the neutron-rich Be isotopes versus the sum of the mass of the decay fragments [A]. The neutron cross-sections are normalized by dividing by the difference in the number of neutrons between the observed fragment and the projectile. The vertical dotted lines indicate the mass of the projectile. *right* (a) The first-chance cluster breakup cross sections, i.e. ^{14}Be->^{6}He+^{8}He, ^{12}Be->^{6}He+^{6}He ^{10}Be->^{6}He+^{4}He (b) the total He+He breakup cross sections and (c) the ratio of the first-chance breakup cross-sections to the total breakup cross-section, versus the mass of the projectile [A].

binding energy of the system (as in atomic systems). Consequently, the heavier Be isotopes are bound against alpha-decay. This exchange process gives rise to molecular-type orbitals for the valence neutrons of σ and π character [Fre07a, Oer06]. The ground-state of ^{9}Be ($J^{\pi} = 3/2^{-}$) has a neutron in a π type orbital, whereas the 1.68 MeV, $1/2^{+}$, excited state has σ-character. It is believed that the ground-state of ^{10}Be should have a $(\pi)^2$ neutron configuration, whereas the $(\sigma)^2$ structure has been associated with the first excited 0^{+} state close to 6 MeV. This latter state is associated with a rotational band with a rather extreme moment of inertia which is interpreted in terms of the two valence neutrons interceding between the alpha-clusters [Fre06]. Calculations using the Antisymmetrized Molecular Dynamics (AMD) framework (which is very similar to the Fermionic Molecular Dynamics approach) has allowed a characterisation of the evolution of the cluster structure in the beryllium isotopes – this is shown in Fig. 6. The molecular type configurations are believed to play an important role in the ground states of the nuclei up to the drip-line and thus the degree of clusterisation is thought to be preserved [Kan01].

2.3.2 Previous Measurements

A series of measurements have been performed at GANIL which have been aimed at characterizing the degree of clusterisation in ^{10,11,12,14}Be, ^{14}B and ^{16}C [Ash04a, Ash04b, Ash04c]. These studies involved the measurement of the charged-particle and break-up and neutron-removal cross sections. The charged particle break-up reaction involves an inelastic excitation from the ground state to cluster states close to the break-up threshold and in this way provides a measure of the overlap between the ground-state and cluster states and thus the degree of clusterisation appearing in the ground state. The results from some of these measurements are shown in Fig. 8. The left hand part of the Figure shows the cross sections measured for the four Be isotopes and part a) of the right hand section shows the cluster break-up cross section for ^{10,12,14}Be. These measurements indicate that the cross section for the cluster breakup (first chance) remains relatively constant and thus one would include that the same is true for the degree of clusterisation – as indicated in Fig. 7. However, the reaction mechanism is rather complex and such measurements therefore do not yield an unambiguous understanding of the ground state structure. Here we propose a series of more sensitive measurements of the nature of the ground-states of Be isotopes, which may also be applied to other light systems, in order to characterise the degree of clusterisation as the drip-line is approached.

2.3.3 Proposed Measurements

We propose a series of quasi-free (p,pα) scattering measurements on the nuclei ^{9,10,11,12}Be using the existing LAND/R3B setup in Cave C. The full setup is described in Section 3. The measurements will be performed by scattering the Be projectiles from protons in a CH_2 target (additional measurements with carbon targets will be made to deduce background contributions). The scattered target-like proton will be detected in the target recoil array. Alpha-particles knocked out from the projectile will be detected in quasi-free kinematics in the same array. The differential energy loss in the silicon element will permit the identification of the helium isotope and protons. The detection of projectile-like reaction products and gamma-rays is performed in the usual way.

In the first instance, these measurements will provide quasi-free scattering cross sections. These yield an indication of the probability for the formation of the cluster in the ground-state. The ground-state structure of ^{9}Be is believed to be well understood and will thus provide the reference point. Insight into the wave-function of the alpha-particle within the Be nucleus and how this evolves from one system to the next will be gained by reconstructing the momentum distribution of the knocked out alpha-particles from the measured momenta of protons and alpha-particles or the recoiling fragment.

The coverage and sensitivity of the detection system will permit not just a characterisation of the ground states but also excited states of the Be nuclei. For example, the inelastic excitation through interactions with the target proton will lead to the population of states above the neutron decay threshold. The subsequent neutron-decay of the projectile to gamma-decaying states in the daughter may be used to provide information on the inelastically excited state. For example, the ^{12}Be nucleus excited above the two neutron decay threshold (3.67 MeV) and close to an excitation energy of 10 MeV can decay either to the ^{10}Be ground state or excited states. The latter can be tagged by the detection of gamma-rays in the target recoil array. Two-neutron decays to the ^{10}Be 2^+ state with a $(\pi)^2$ neutron configuration, and the group of excited states close to 6 MeV with a $(\sigma)^2$ or $(\pi)^1(\sigma)^1$ character would help determine the structure of excited states in ^{12}Be which have been observed close to the cluster decay threshold [Fre07b, Cha07]. It should be noted that the cluster knockout can also be measured on all of the projectiles present in the FRS setting. This experiment would thus consitute the most comprehensive study ever undertaken in neutron-rich nuclei.

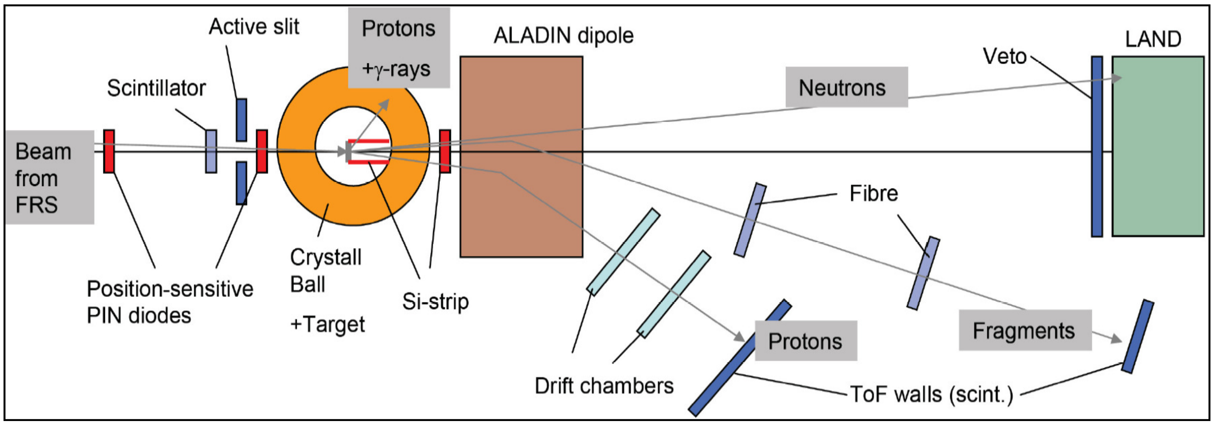

Figure 9. Schematic view of the experimental setup (not to scale). Active Slit: 4-jaw slit, organic scintillator, remote control, vetoing beam halos; Start : thin organic scintillator, time of flight ($\sigma_{tof} \sim 30$ ps); PIN : pin silicon diode, 5×5 cm^2, 2-dim. Position readout ($\sigma_{x,y} \sim 30$ mm), energy-loss ($\sigma_Z \sim 0.2e$); Fibre: scintillating fibre array, 50×50 cm^2, 500 fibres; Target Recoil Detector : micro-strip Si detector array to track and identify qfs protons; Crystal Ball: segmented NaI detector, γ-ray and qfs proton detection in $\sim 4\pi$; ALADIN: Large gap dipole magnet; Veto/LAND: neutron-detector, 2×2 m^2, ($\sigma_{tof} \sim$ 200 ps; $\sigma_{x,y} \sim 3$ cm); ToF : array 14 + 18 organic scintillators, 1.8×1.4 m^2, , ($\sigma_{tof} \sim 100$ ps), energy-loss measurement

3. Experimental Technique

The existing LAND/R3B set-up in Cave C will be used for the Coulomb breakup and quasifree scattering experiments. It provides tracking, unique identification and momentum determination for the incoming secondary beam and also the outgoing forward focused projectile residues, heavy fragments and light charged particles. The unambiguous identification of the residual fragment selects the correct reaction channel and so reduces strongly the influence from other reaction channels and multiple scattering. The setup also allows for measurements of the momentum and position of the kinematically forward-focused neutrons. An additional tagging of the originating state can be achieved by detecting gamma rays from the resulting nucleus.

The main experimental tasks are: identification and determination of the momentum of the components of the mixed secondary beam delivered by the FRS, identification and determination of the momentum before and after the reaction in the target and detection of all decay products. This will be accomplished by means of energy loss and position measurements with position sensitive pin diodes, a time-of-flight measurement over a large distance between the FRS and the experimental area, and from the magnetic rigidity determined at the FRS. The heavy fragments emerging after dissociation in the target will be again identified ($\sigma_Z \approx 0.2$; $\sigma_A \approx 0.2$) and momentum analyzed using position sensitive pin diodes placed in between the target and the ALADIN magnet, and using scintillating fiber arrays and a time-of-flight wall (1.8×1.4 m^2) consisting of 32 position sensitive organic scintillator paddles. Neutrons and γ-rays will be detected in LAND and the Crystal Ball detector, respectively. The excitation energy spectra can be obtained from an invariant-mass analysis involving the fragment, neutrons and γ-rays. Resolutions of 0.2 – 3 MeV (FWHM) can be achieved, depending on excitation energy.

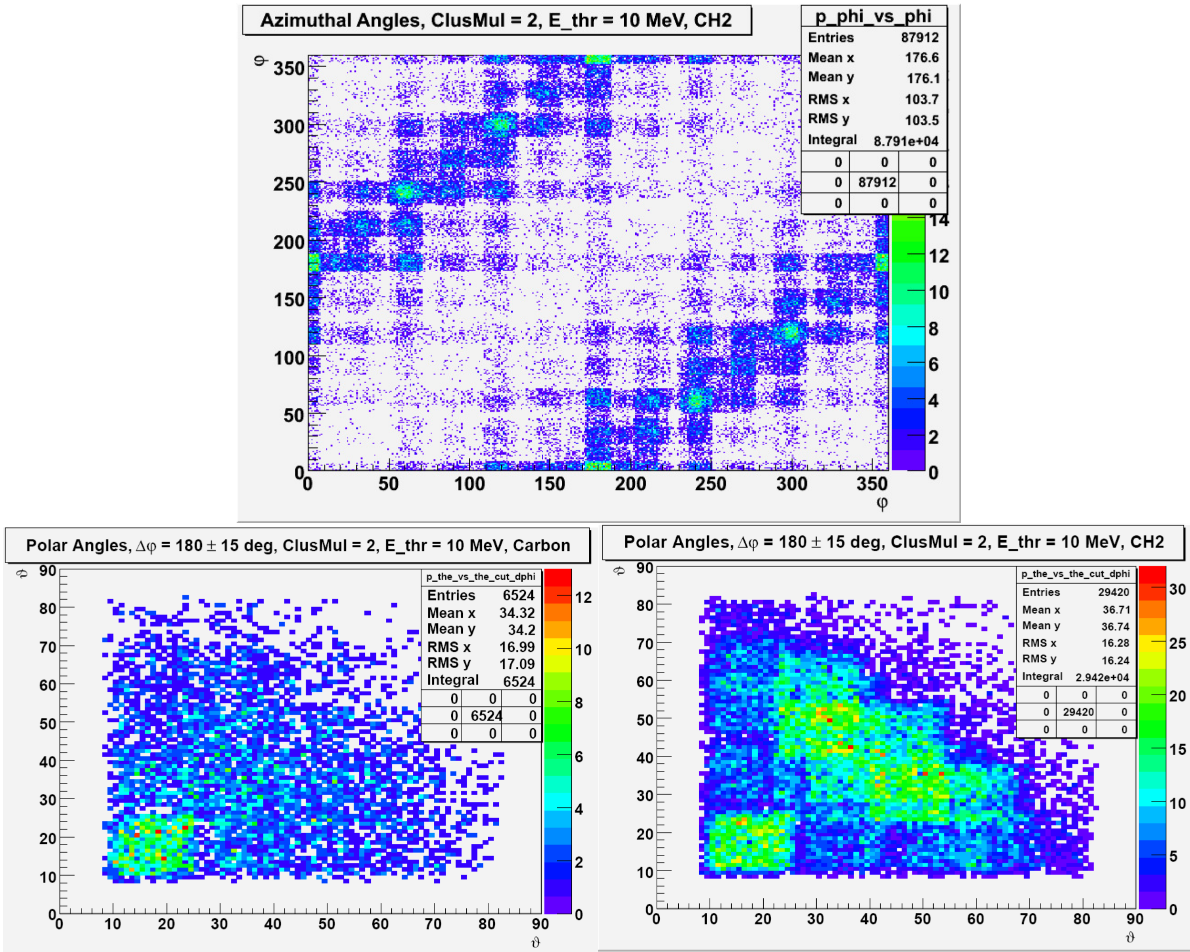

Figure 10. Correlation plots for two-proton events in the reaction of ^{17}Ne to oxygen. The upper plot shows the azimuthal angular correlation among the two protons. The correlation pattern correspond to an angle difference of approximately 180 º. The two lower plots show the angular correlations in the polar angle for the two targets C (left) and CH_2 (right). From [Wam08].

The outgoing protons (and deuterons or alphas) will be tracked and identified by a target recoil detector consisting of high-resolution Si micro-strip detectors and the Crystal Ball. The Si micro-strip detectors will be placed in the forward direction surrounding the beam pipe and at zero degrees, covering an angular range of 0° - 80°, which spans the full decay cone expected for single-step quasi-free nucleon knockout. This layer, together with the beam tracking onto the target and the Crystal Ball detectors, will allow tracking of the protons as they leave the target and reconstruction of the reaction vertex and, in addition, provide an energy loss measurement. The following layer is provided by the Crystal Ball (162 NaI Crystals, 25 cm long) to detect the protons and provide an energy measurement. The second role of the scintillating crystals will be to act as a total absorption gamma-ray spectrometer. This will allow us to tag hole-states (if particle-bound) in the nucleus being probed by their characteristic gamma-ray energies. Thus this layer must be capable of detecting protons with energies of 100-400 MeV in the laboratory system and gamma rays of order 1 MeV. This is accomplished by a modified read-out of the PM-tubes to allow two different ranges.

The setup has been used previously to study quasi-free knockout reactions. In an experiment devoted to the structure of the two-proton halo nucleus ^{17}Ne, a run with a CH2 target was taken and the scattered protons have been detected using the above mentioned target recoil detector. The data are currently being analyzed. Fig. 10 shows preliminary results of the angular correlations for two-proton events observed in the Crystal Ball alone. Plotted are the two azimuthal angles of the protons determined from the granularity of the Crystal Ball (events have been randomized within the uncertainty of ±7.5º). A clear correlation pattern is visible corresponding to events with a difference in angle of about 180º, typical for quasi-free scattering events. In the lower part the correlations in polar angle are shown for the two targets, C and CH_2. For the latter target, a clear correlation is observed corresponding to two protons with a mean opening angle of around 82º. This is result is in good agreement with the simulated result of 84º for quasi-free proton knockout from ^{17}Ne. The data clearly indicate that the typical kinematical correlations of QFS events can be selected by the setup. The remaining background, stemming from the carbon in the CH_2 target, can be subtracted. Eventually, the angle of the protons will be more precisely determined by measurements with the Si strip detectors and the total energy will be measured using the Crystal Ball. This information will allow the reconstruction of both the separation energy of the knocked-out nucleon (or cluster) as well as the intrinsic momentum distribution. As mentioned before, the same information can be obtained from the heavy fragment, thus yielding redundant information on energy and momentum.

4. Rate Estimates

Rate estimates were calculated using the Lise++ code with the parameters shown in Table 1 and the resulting secondary beam intensities can be seen in Table 2. The rate estimates are based on production cross sections calculated with EPAX 2.15 [Sum00], except for the ^{18}C case, where the experimental cross section has been used. The expected maximum primary beam intensity impinging on the FRS target is $1.5x10^{10}$ ions/spill as known from previous experiments. The rates given in Table 2 are per 10^{10} ^{40}Ar ions on target. The maximum average intensity per second is reached with fast ramping and a rather short spill of 1 sec resulting in a total cycle time of about 3 sec. This mode will be used for the most exotic settings with low rate. The resulting average intensity is then the one given in the table divided by two.

Table 1: Parameters used for Lise++ calculations.

Primary beam	600 *A*MeV ^{40}Ar
Primary beam intensity	10^{10} ^{40}Ar
Target thickness	Be: 4011 mg/cm^2
Wedge at S2	2000 mg/cm^2
Scintillator S2	3 mm
Scintillator S8	3 mm

Table 2. Secondary beam intensities at the Cave C target per 10^{10} ^{40}Ar ions impinging on the FRS target. Rates have been estimated with Lise++ using EPAXII cross sections and realistic beam transport to Cave C. (600 MeV/u, 4 g/cm^2 Be target, 2g/cm^2 Al degrader at S2).

Intensity	(sett.1)	(sett.2)	(sett.3)	(sett.4)	(sett.5)	(sett.6)
^{9}Be		8480	5770	-	-	-
^{10}Be	-	-	2.0e+4	2380	36	-
^{11}Be	-	-	76	4250	3550	636
^{12}Be	-	-	-	18	22	616
^{14}B	-	-		962	1290	246
^{15}B	-	-	-	1.8	44	146
^{15}C			1.6e+4	253		
^{16}C			156	2250	153	
^{17}C	-	-		172	341	60
^{18}C	-	-	-	0.3	10	29
^{13}O	48					
^{14}O	1.4e+4					
^{15}O	6570		-	-	-	-
^{16}O	-	2.8e+4	-	-	-	-
^{17}O	-	4.0e+5	-	-	-	-
^{18}O	-	2.5e+4	14	-	-	-
^{19}O	-	5	1.e+4	-	-	-
^{20}O	-	-	1.3e+4	0.5	-	-
^{21}O	-	-	25	258	0.04	-
^{22}O		-	3.e-2	195	38	0.3e-2
^{23}O		-	-	3	17	3.4
^{24}O		-	-	-	0.2	1.2
^{17}F	4030					
^{18}F	-	1.6e+4	-	-	-	-
^{19}F	-	5.5e+5	-	-	-	-
^{20}F	-	1.0e+5	-	-	-	-
^{21}F	-	104	1150	-	-	-
^{22}F	-	-	1.8e+4	-	-	-
^{23}F	-	-	2530	4	-	-
^{24}F	-	-	7	250	0.4	-
^{25}F	-	-	-	45	17	0.01
^{26}F		-	-	0.2	4	0.9
^{27}F		-		-	0.03	0.3
^{17}Ne	422					
^{18}Ne	1.4e4					
^{19}Ne	1970					
^{20}Ne	-	4.6e+3	-	-	-	-
^{21}Ne	-	6.2e+5	-	-	-	-
^{22}Ne	-	2.4e+5	-	-	-	-
^{23}Ne	-	624	11	-	-	-
^{24}Ne	-	-	8870	-	-	-
^{25}Ne	-	-	1.e+4	-	-	-
^{26}Ne	-	-	204	28	-	-
^{27}Ne	-	-		114	0.3	-
^{28}Ne	-	-	-	8	6	-
^{29}Ne	-	-	-		0.9	0.3

For the Coulomb dissociation measurement with setting 6, 10 shifts with Pb target are foreseen (see Section 1). In addition, measurements have to be made with a carbon target in order to estimate the nuclear contribution to the cross section measured with Pb. Empty target measurements serve to subtract background originating from reaction outside the target.

The inclusive cross section for a (p,2p) reaction amounts to about 10 mb. With a 200 mg/cm^2 thick CH_2 target, we expect to collect about 100,000 events in a day for the settings with high rates, i.e., up to ^{20}O. For theses cases, precise measurement of exclusive spectral functions will be possible. For the neutron-rich settings, thicker targets will be used. The most neutron-rich setting, which will be used for the ^{18}C (γ,n) measurements, contains also 1.2 ^{24}O per 10^{10} ^{40}Ar ions in the mixed beam. Making use of the fast-ramping mode and a 1 sec extraction time, an average intensity of 0.6/sec is expected. With a 1 g/cm^2 CH_2 target, a total yield of about 250 events is expected in 10 shifts. At the same time, alpha knockout from ^{12}Be and the ^{27}F(p,2p)^{26}O reaction will be studied. In the latter case, the statistics from C and H (~100 events) in the CH_2 as well as from the C measurement (which is needed for the Coulomb dissociation measurement) can be added. This will be sufficient to locate the ground state of ^{26}O and determine its width.

A summary of the beamtime request for the different settings and targets is given in Table 3.

Table 3. A summary of the beamtime request for the different settings and targets.

	setting 1	**setting 2**	**setting 3**	**setting 4**	**setting 5**	**setting 6**	Physics
A/Z	**1.75**	**2.12**	**2.5**	**2.75**	**2.88**	**3.0**	
example nuclei of interest	$^{13-15}$O	$^{16-18}$O ^{9}Be	^{19,20}O ^{10}Be	^{21,22}O ^{11}Be	^{23}O ^{11}Be ^{17}C,^{14}B	^{18}C ^{24}O ^{12}Be ^{26,27}F	Astro p,2p p,pα unbound
target							
Pb	-	-	-	-	-	10	
C	1	1	1	2	2	3	
empty	1	1	1	2	2	4	
CH2	3	3	3	6	6	10	
setting FRS	1	1	1	1	1	1	Total
	6	6	6	11	11	28	58

In addition, we need 2 days prior to the main run for setting up the LAND/R3B setup in Cave C and for calibration measurements. In total, we ask for 21 days of beam time.

The collaboration plans to perform the experiment in 2010.

References

[Aks08] Yu. Aksyutina et al., Phys. Lett. B 666 (2008) 430.
[Aks09a] Yu. Aksyutina et al., GSI experiment S245, to be published.
[Aks09b]Yu. Aksyutina et al., “Beyond the dripline: Helium isotopes”, draft in press.
[Ash04a] N.I. Ashwood, et al. Phys. Lett. B 580 (2004) 129.
[Ash04b] N.I. Ashwood et al., Phys. Rev. C 70 (2004) 064607.
[Ash04c] N.I. Ashwood et al., Phys. Rev. C 70 (2004) 024608.
[Bar08] C. Barbieri and W.H. Dickhoff, Proceedings of the “KGU Yokohama Autumn School of Nuclear Physics”, October 2008; arXiv:0901.1920v1.
[Baz03] D. Bazin et al., Phys. Rev. Lett. 91 (2003) 012501.
[Cha07] R. Charity, et al., Phys. Rev. C 76 (2007) 064313.
[Fre06] M. Freer, et al., Phys. Rev. Lett. 96 (2006) 042501.
[Fre07a] M. Freer, Rep. Prog. Phys. 70 (2007) 2149.
[Fre07b] M. Freer et al., Phys. Rev. Lett. 82 (1999) 1383.
[Fri05] T. Frick et al., Phys. Rev. C 71 (2005) 014313.
[Gad08] A. Gade et al., Phys. Rev. C 77 (2008) 044306.
[Hof08] C.R.Hoffman et al., Phys.Rev.Lett. 100 (2008) 152502.
[Kan01] Y. Kanada En’yo and H. Horiuchi, Prog. Theo. Phys. 142 (2001) 205.
[Lec09] J.-L. Lecouey et al., Physics Letters B 672 (2009) 6.
[Mei02] M. Meister et al., Phys. Rev. Lett., 88 (2002) 102501.
[Mey92] B.S. Meyer et al., Astrophys. J. 399 (1992) 656.
[Mou80] J. Mougey, Nucl. Phys. A 335 (1980) 35.
[Oer06] W. von Oertzen, M. Freer and Y. Kanada En’yo, Physics Reports 432 (2006) 43.
[Oza00] A. Ozawa et al., Nucl. Phys. A 673 (2000) 411.
[Sas05] T. Sasaqui et al., Astrophys. J. 634 (2005) 1173.
[Sim08] H. Simon et al., Nucl. Phys. A 810 (2008) 267.
[Sne03] C. Sneden et al., Astrophys. J. 591 (2003) 936.
[Sum00] K. Sümmerer and B. Blank, Phys. Rev. C 61 (2000) 034607.
[Ter01] M. Terasawa et al., Astrophys. J. 562 (2001) 470.
[Wam08] F. Wamers, PhD thesis, Technical University Darmstadt
[Wir00] R. B. Wiringa et al., Phys. Rev. C 62 (2000) 014001.
[Woo94] S.E. Woosley et al., Astrophys. J. 433 (1994) 229.